Journal of Applied Mechanics and Technical Physics, Vol. 47, No. 2, pp. 282–288, 2006

ANALYSIS OF PLANE PHASE STRAINS OF RODS AND PLATES

L. I. Shkutin

UDC 539.370

The problem of a rod and a plate subjected to plane strain in the interval of the direct phase transformation is formulated as a nonlinear boundary-value thermoelastic problem with an implicit dependence on temperature (through a phase parameter simulating the volume fraction of new-phase crystals). An analytical solution of the problem of a rod bent into a ring and a plate bent into a tube as a result of phase strains under the action of a small end bending moment is given. A numerical analysis of the buckling problem of a titanium nickelide (alloy) rod (plate) under longitudinal compression in the interval of the direct phase transformation shows that buckling becomes possible if the compressive load is much lower than the Euler critical load calculated before the transformation. Branches of buckled equilibrium states corresponding to loads lower than the Euler load are plotted as functions of the phase parameter. In all cases considered, the deflections increase abruptly in the neighborhood of the critical points. The evolution of buckling modes is studied, and the phase-strain distributions along the rod (plate) are shown.

Key words: *shape-memory alloys, rods, plates, phase strains, buckling, numerical analysis.*

Metal alloys undergoing phase transformations under thermal cycling are mainly used in design of thermosensitive structural elements. Thin-walled elements made of these alloys exhibit a very pronounced shape-memory effect. Unique mechanical properties of shape-memory alloys are determined by their thermoelastic phase transformations. Cooling of a loaded specimen in the phase-transformation interval results in the phase strain whose deviator is proportional to the internal-stress deviator at a constant temperature. Under subsequent heating of the specimen in the inverse-transformation interval, the phase strain acquired earlier is removed partly or completely (which is called the shape-memory effect). Over the last years, a certain progress has been achieved in constructing mathematical equations modeling the phase-transformation and shape-memory effects. In the present paper, micromechanical constitutive relations proposed and justified in [1, 2] are used. In [3], these equations were applied to some nonlinear bending problems of rods in the direct-transformation interval, including the buckling problems. It was found [3] that, within the temperature interval of martensite transformation, intense buckling of a rod occurs under a compressive load lower than the Euler load if a very small transverse force is applied to the rod end. The possibility of buckling of a compressed rod and a plate is established below by a numerical analysis of branching of the solutions of the corresponding nonlinear boundary-value problem. Moreover, an analytical solution of the problem of a rod bent into a ring and a plate bent into a tube owing to phase strains is obtained. The solutions of the problems considered are obtained by the kinematic model of a rod with independent rotations of its cross sections [4].

Plane-Strain Equations of Rods and Plates. Let x_J ($J = 1, 2, 3$) be a Cartesian coordinate system to which the motion of material points of the deformed rod is referred and $\boldsymbol{i}_J$ be an orthonormal basis of this system. A local coordinate system t_J with an orthonormal basis $\boldsymbol{e}_J^0(t_3)$ is related to the reference line of the rod in such a manner that t_3 is the internal parameter of the line and t_1 and t_2 are the transverse coordinates.

Institute of Computer Modeling, Siberian Division, Russian Academy of Sciences, Krasnoyarsk 660036; shkutin@icm.krasn.ru. Translated from Prikladnaya Mekhanika i Tekhnicheskaya Fizika, Vol. 47, No. 2, pp. 156–164, March–April, 2006. Original article submitted June 29, 2005.

We consider a rod with a plane reference line whose undeformed configuration is determined by the parametric equations

$$\boldsymbol{x} = x_2\boldsymbol{i}_2 + x_3\boldsymbol{i}_3, \quad x_2 = x_2(t_3), \quad x_3 = x_3(t_3) \qquad \forall\, t_3 \in [0, l] \tag{1}$$

[$\boldsymbol{x}(t_3)$ is the position vector of an arbitrary point and l is the length of the line]. According to (1), the reference line is located in the coordinate plane with the basis $(\boldsymbol{i}_2, \boldsymbol{i}_3)$.

The orthonormal bases $\boldsymbol{i}_J$ and $\boldsymbol{e}^0_J(t_3)$ can be interrelated by the orthogonal transformation $\boldsymbol{e}^0_J = \boldsymbol{i}_J \cdot \boldsymbol{O}^0$ with the rotator tensor $\boldsymbol{O}^0(t_3)$ whose components are determined in both bases by the orthogonal matrix

$$O^0_{JK} = \begin{bmatrix} 1 & 0 & 0 \\ 0 & \cos\theta_0 & \sin\theta_0 \\ 0 & -\sin\theta_0 & \cos\theta_0 \end{bmatrix} \tag{2}$$

[$\theta_0(t_3)$ is the angle of rotation of the basis $\boldsymbol{e}^0_J(t_3)$ about the vector $\boldsymbol{i}_1$].

By definition, the relations $dx_2/dt_3 = -\sin\theta_0$ and $dx_3/dt_3 = \cos\theta_0$ are valid, and the vector $\boldsymbol{y} = \boldsymbol{x} + t_i\boldsymbol{e}^0_i$ $(i = 1, 2)$ defines the coordinates of an arbitrary point of the rod.

We consider the plane strain of the rod such that, during deformation, the reference line remains plane and is determined by the position vector

$$\boldsymbol{a} = a_2\boldsymbol{i}_2 + a_3\boldsymbol{i}_3, \quad a_2 = a_2(t_3), \quad a_3 = a_3(t_3) \qquad \forall t_3 \in [0, l] \tag{3}$$

(a_2 and a_3 are the unknown coordinates of the point t_3).

Using the orthogonal transformation

$$\boldsymbol{e}_J = \boldsymbol{i}_J \cdot \boldsymbol{O} = \boldsymbol{e}^0_J \cdot \bar{\boldsymbol{O}}^0 \cdot \boldsymbol{O} \tag{4}$$

with the rotator tensor $\boldsymbol{O}(t_3)$, we introduce a local orthonormal basis $\boldsymbol{e}_J(t_3)$ rotating during deformation ($\bar{\boldsymbol{O}}^0$ is the tensor conjugate to $\boldsymbol{O}^0$). In the bases $\boldsymbol{i}_J$ and $\boldsymbol{e}_J$, the components of the rotator $\boldsymbol{O}$ are determined by a matrix of the form of (2):

$$O_{JK} = \begin{bmatrix} 1 & 0 & 0 \\ 0 & \cos\theta & \sin\theta \\ 0 & -\sin\theta & \cos\theta \end{bmatrix}. \tag{5}$$

Here $\theta = \theta_0 + \vartheta$ is the angle of rotation of the basis $\boldsymbol{e}_J$ about $\boldsymbol{i}_1$ and $\vartheta(t_3)$ is the increment in the rotation angle owing to deformation. In the initial state, $\vartheta \equiv 0$, and the basis $\boldsymbol{e}_J$ coincides with $\boldsymbol{e}^0_J$. The local rotation given by matrix (5) has only one degree of freedom: angle of rotation θ or $\vartheta = \theta - \theta_0$.

In a deformed state, the location of an arbitrary point of the rod is determined by the vector [4]

$$\boldsymbol{g} = \boldsymbol{a} + t_i\boldsymbol{e}_i \qquad (i = 1, 2). \tag{6}$$

This basic kinematic approximation specifies the motion of each cross section as a rigid body with two translational degrees of freedom $a_2(t_3)$ and $a_3(t_3)$ and one rotational degree of freedom $\theta(t_3)$. Function (6) corresponds to the linear dependence of the three-dimensional displacement field on the transverse coordinates

$$\boldsymbol{w} \equiv \boldsymbol{g} - \boldsymbol{y} = \boldsymbol{u} + t_i(\boldsymbol{e}_i - \boldsymbol{e}^0_i), \qquad \boldsymbol{u} \equiv \boldsymbol{a} - \boldsymbol{x}. \tag{7}$$

The volume strain vectors $\boldsymbol{w}_J = \boldsymbol{g}_{,J} - \boldsymbol{y}_{,J} \cdot \boldsymbol{O}$ (see [4]) are calculated by means of Eq. (6):

$$\boldsymbol{w}_3 = \boldsymbol{u}_3 + t_2\,\boldsymbol{v}_3, \qquad \boldsymbol{w}_i = \boldsymbol{0}. \tag{8}$$

Here the following contour vectors of the metric and bending strains are introduced:

$$\boldsymbol{u}_3 \equiv \boldsymbol{a}_{,3} - \boldsymbol{e}_3, \qquad \boldsymbol{v}_3 \equiv \boldsymbol{e}_{2,3} - \boldsymbol{e}^0_{2,3} \cdot \boldsymbol{O}. \tag{9}$$

To formulate scalar kinematic equations, we use the following expansions, which agree with Eqs. (4) and (5):

$$\boldsymbol{e}_1 = \boldsymbol{i}_1, \qquad \boldsymbol{e}_2 = \boldsymbol{i}_2\cos\theta + \boldsymbol{i}_3\sin\theta, \qquad \boldsymbol{e}_3 = -\boldsymbol{i}_2\sin\theta\ + \boldsymbol{i}_3\cos\theta. \tag{10}$$

We understand formula (9) determining the metric-strain vector as an equation for the unknown position vector $\boldsymbol{a}$. Substituting $\boldsymbol{u}_3$ written as $\boldsymbol{u}_3 = u_{32}\boldsymbol{e}_2 + u_{33}\boldsymbol{e}_3$ into (9), and combining (3) and (10), we obtain the scalar equations

$$a_{2,3} = u_{32}\cos\theta - (1 + u_{33})\sin\theta, \qquad a_{3,3} = u_{32}\sin\theta + (1 + u_{33})\cos\theta. \tag{11}$$

Taking into account Eqs. (9) and (10), we infer that the bending-strain vector $\boldsymbol{v}_3$ has only one component:

$$v_{33} = \boldsymbol{v}_3 \cdot \boldsymbol{e}_3 = \theta_{,3} - \theta_{0,3}, \qquad v_{32} = \boldsymbol{v}_3 \cdot \boldsymbol{e}_2 = 0. \tag{12}$$

The stress state of the rod, induced by the action of strain, is measured by the stress vector $\boldsymbol{s}_3 = S_{32}\boldsymbol{e}_2 + S_{33}\boldsymbol{e}_3$, which acts on the unit area of the undeformed cross section. Here S_{32} is the transverse shear stress and S_{33} is the compressive or tensile normal stress.

The resulting stress vectors are given by the inequalities

$$\boldsymbol{t}_3 = \int_A \boldsymbol{s}_3 J \, dA, \qquad \boldsymbol{m}_3 = \int_A \boldsymbol{s}_3 J t_2 \, dA. \tag{13}$$

For the smooth force fields $\boldsymbol{t}_3(t_3)$ and $\boldsymbol{m}_3(t_3)$, the following dynamic equations are satisfied at the reference line [4]:

$$\boldsymbol{t}_{3,3} + \boldsymbol{p} = \boldsymbol{0}, \qquad (\boldsymbol{e}_2 \times \boldsymbol{m}_3)_{,3} + \boldsymbol{a}_{,3} \times \boldsymbol{t}_3 + \boldsymbol{q} = \boldsymbol{0}. \tag{14}$$

Here $\boldsymbol{p}(t_3)$ and $\boldsymbol{q}(t_3)$ are the vectors of external forces and moments distributed along the rod.

In Eqs. (14), we write $\boldsymbol{t}_3$, $\boldsymbol{m}_3$, and $\boldsymbol{a}_{,3}$ as

$$\boldsymbol{t}_3 = T_{32}\,\boldsymbol{e}_2 + T_{33}\,\boldsymbol{e}_3 = T_2\,\boldsymbol{i}_2 + T_3\,\boldsymbol{i}_3, \quad \boldsymbol{m}_3 = M_{32}\,\boldsymbol{e}_2 + M_{33}\,\boldsymbol{e}_3, \quad \boldsymbol{a}_{,3} = u_{32}\,\boldsymbol{e}_2 + (1 + u_{33})\,\boldsymbol{e}_3$$

and obtain the dynamic equations in a scalar form

$$\begin{gathered} T_{2,3} + P_2 = 0, \quad T_{3,3} + P_3 = 0, \quad M_{33,3} + u_{32}T_{33} - (1 + u_{33})T_{32} + Q_1 = 0, \\ T_{32} = T_2 \cos\theta + T_3 \sin\theta, \qquad T_{33} = -T_2 \sin\theta + T_3 \cos\theta. \end{gathered} \tag{15}$$

Here T_{32}, T_{33}, M_{32}, and M_{33} are the components of the internal forces and moments in the rotated coordinate system, T_2 and T_3 are the Cartesian components of the force vector, and P_2, P_3, and Q_1 are the Cartesian components of the external forces and moments.

Equations (11), (12), and (15) constitute a system of nonlinear kinematic and dynamic equations of the deformed rod.

Constitutive Relations. To find the stress–strain relation in the interval of the direct phase transformation, we use the system of micromechanical constitutive relations [1]

$$\begin{gathered} w_{32} = \varphi_{32} + S_{32}/G, \qquad w_{33} = \varphi_{33} + S_{33}/E, \\ d\varphi_{32} = (\varkappa_0 \varphi_{32} + S_{32}/\sigma_0)\, dq, \qquad d\varphi_{33} = (\varkappa_0 \varphi_{33} + (2/3)S_{33}/\sigma_0)\, dq, \\ q = \sin\Big(\frac{\pi}{2}\,\frac{T_+ - T}{T_+ - T_-}\Big), \qquad T_- \leqslant T \leqslant T_+, \quad 0 \leqslant q \leqslant 1. \end{gathered} \tag{16}$$

Here E and G are the tensile–compressive and shear elastic moduli, respectively, $\varkappa_0$ and σ_0 are the experimental constants of the alloy in the direct phase transformation interval, $\varphi_{32}(t_3)$ and $\varphi_{33}(t_3)$ are the phase strains, q is the internal parameter of state determined as the volume fraction of the martensite phase, T_+ and T_- are the initial and final temperatures of the direct transformation, respectively, and T is the current temperature. In the relations given above, the thermal strain of the alloy and the volume effect of phase transformation are ignored; therefore, φ_{32} and φ_{33} are, in essence, the components of the phase-strain deviator. In addition, we assume that the phase transformation is an isothermal process with a uniform temperature distribution over the specimen volume, which implies that the parameter q is independent of coordinates.

It follows from Eq. (16) that the phase strains are determined by differential (with respect to the parameter q) equations. The first terms in their right sides are responsible for the development of martensite crystals and the second terms take into account the nucleation and orientation of the crystals in the direction of acting stresses. The elastic moduli in (16) vary in the phase-transformation interval from their austenite values to their martensite values. Bearing in mind the meaning of the parameter q, we represent these moduli in the phase-transformation interval as the Voigt-averaged relations [2]

$$E = qE_- + (1 - q)E_+, \qquad G = qG_- + (1 - q)G_+,$$

where the subscripts minus and plus refer to the martensite and austenite phases, respectively.

Assuming that the stresses depend on the parameter q much weaker than the phase strains, we obtain an approximate solution of the differential equations (16):

$$\varphi_{32} \simeq \frac{S_{32}}{\sigma_0 \varkappa_0} (\exp(\varkappa_0 q) - 1), \qquad \varphi_{33} \simeq \frac{2}{3} \frac{S_{33}}{\sigma_0 \varkappa_0} (\exp(\varkappa_0 q) - 1). \tag{17}$$

This solution satisfies the physical conditions: the phase strains vanish in austenite (for $q = 0$) and reach a maximum value in martensite (for $q = 1$).

Substituting functions (17) into the first and second equations of system (16), we obtain the approximate constitutive relations

$$w_{32} \simeq \gamma_2 S_{32}/E_0, \qquad w_{33} \simeq \gamma_3 S_{33}/E_0,$$
$$\gamma_2(q) \equiv \frac{E_0}{G} + \frac{E_0}{\sigma_0 \varkappa_0} (\exp(\varkappa_0 q) - 1), \qquad \gamma_3(q) \equiv \frac{E_0}{E} + \frac{2}{3} \frac{E_0}{\sigma_0 \varkappa_0} (\exp(\varkappa_0 q) - 1). \tag{18}$$

Here E_0 is a constant with the dimension of stress, which is conveniently identified with E_- or E_+.

Equations (18) represent the phase transformation as thermoelastic strain with an implicit dependence on temperature (through the parameter q).

According to Eqs. (8) and (12), we obtain $w_{32} = u_{32}$ and $w_{33} = u_{33} + t_2 v_{33} = u_{33} + t_2(\theta - \theta_0)_{,3}$. Substituting these expressions into (18) and integrating over the cross section of the rod, with allowance for (13), we obtain the resulting constitutive relations

$$u_{32} \simeq \gamma_2 T_{32}/(AE_0), \qquad u_{33} \simeq \gamma_3 T_{33}/(AE_0), \qquad \theta_{,3} - \theta_{0,3} \simeq \gamma_3 M_{33}/(IE_0), \tag{19}$$

where A is the cross-sectional area and I is the cross-sectional moment of inertia about the vector $\boldsymbol{e}_1^0$.

Equations (11), (12), (15), and (19) constitute a closed system of six first-order differential equations whose solution depends on the parameter q. In numerical integration of the system, its solutions are found for discrete values of the parameter q within the interval $0 \leqslant q \leqslant 1$. The last expression in (16) relates the parameter q to the temperature of the alloy.

The system formulated above also models the plane strain of plates and panels undergoing thermoelastic phase transformations.

Dimensionless Formulation of the System of Equations. We introduce an independent argument $t = t_3/l$, a geometrical parameter $\varepsilon^2 = I/(Al^2)$, external-force parameters $p_2 = P_2 l^3/(IE_0)$, $p_3 = P_3 l^3/(IE_0)$, and $q_1 = Q_1 l^2/(IE_0)$, and unknown functions

$$y_0 = \theta, \quad y_1 = M_{33} l/(IE_0), \quad y_2 = a_2/l, \quad y_3 = a_3/l, \quad y_4 = T_2 l^2/(IE_0), \quad y_5 = T_3 l^2/(IE_0).$$

Now system (11), (12), (15), (19) can be written in dimensionless form

$$y_0' = \gamma_3 y_1 + \theta_0', \quad y_1' = f_2 + (\gamma_3 - \gamma_2)\varepsilon^2 f_2 f_3, \quad y_2' = -\sin y_0 + \varepsilon^2(\gamma_2 f_2 \cos y_0 - \gamma_3 f_3 \sin y_0),$$
$$y_3' = \cos y_0 + \varepsilon^2(\gamma_2 f_2 \sin y_0 + \gamma_3 f_3 \cos y_0), \quad y_4' = -p_2, \quad y_5' = -p_3, \tag{20}$$
$$f_2 \equiv y_4 \cos y_0 + y_5 \sin y_0, \quad f_3 \equiv -y_4 \sin y_0 + y_5 \cos y_0.$$

Here γ_2 and γ_3 are the parameters of state of the alloy [see (18)]; the prime denotes differentiation with respect to t. The boundary conditions for system (20) are formulated in particular problems.

The solutions of the boundary-value problems given below were obtained for rods and plates made of a titanium nickelide alloy with the following experimental values of the parameters of the thermoelastic martensite transformation [2]: $T_- = 25°\text{C}$, $T_+ = 50°\text{C}$, $E_- = 28$ GPa, $E_+ = 84$ GPa, $E_0 = E_+$, $\sigma_0 = 0.049E_+$, $\varkappa_0 = 0.718$, $\nu_- = 0.48$, and $\nu_+ = 0.33$ (ν_- and ν_+ are Poisson's ratios for the martensite and austenite phases, respectively).

Bending of a Straight Rod and a Plate by an End Moment. In the coordinate system chosen in the present paper, a straight rod should be oriented along the x_3 coordinate and a plate should be aligned in the (x_3, x_1) plane so that $\theta_0 = 0$. Let l be the length of the rod or plate in the x_3 direction. For plane bending of a cantilevered rod (plate) by an end moment M, there are no external distributed loads ($P_2 = P_3 = Q_1 = 0$), and system (20) becomes

$$y_0' = \gamma_3 y_1, \quad y_1' = 0, \quad y_2' = -\sin y_0, \quad y_3' = \cos y_0, \quad y_4' = 0, \quad y_5' = 0 \quad \forall t \in (0, 1). \tag{21}$$

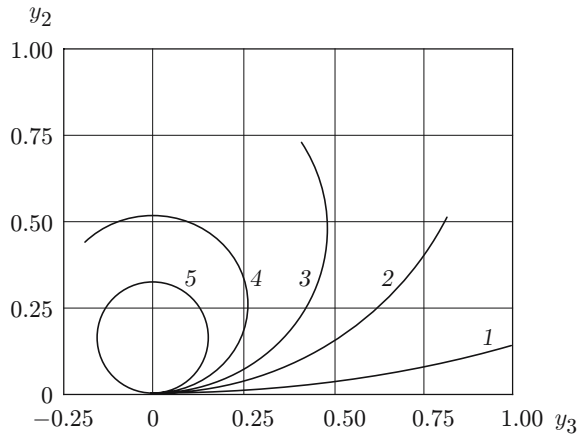

Fig. 1. Evolution of the bent shapes of the rod (plate) for $q = 0$ (1), 0.2 (2), 0.4 (3), 0.7 (4), and 1.0 (5).

The conditions of the clamped end $x_3 = 0$ and the constraint-free end $x_3 = l$ are given by

$$y_0(0) = 0, \quad y_2(0) = 0, \quad y_3(0) = 0, \quad y_1(1) = -\mu, \quad y_4(1) = 0, \quad y_5(1) = 0, \tag{22}$$

where $\mu = Ml/(IE_0)$ is the numerical parameter of the specified end moment; the bracketed values are the boundary values of the argument t.

The boundary-value problem (21), (22) has the exact solution

$$y_5 = y_4 = 0, \quad y_1 = -\mu, \quad y_0 = \theta = -\mu\gamma_3 t, \quad y_2 = \frac{1 - \cos(\mu\gamma_3 t)}{\mu\gamma_3}, \quad y_3 = \frac{\sin(\mu\gamma_3 t)}{\mu\gamma_3},$$

which shows that the bent rod (plate) is a circular arc of radius $l/(\mu\gamma_3)$ centered at the point $x_2 = l/(\mu\gamma_3)$, $x_3 = 0$; the internal bending moment $M_{33} = -M = -\mu E_0 I/l$ being constant along the arc. The arc becomes a circumference provided that $\mu = 2\pi/\gamma_3$. This value of μ depends on q and other internal parameters of the material. It reaches a minimum value with respect to q for $q = 1$: $\mu_- = 2\pi/\gamma_3(1) \simeq 0.274$.

Figure 1 shows the evolution of the bent shapes of the rod (plate) for different values of q and $\mu = 0.274$. The rod is bent into a ring and the plate is bent into a tube of radius $l/(2\pi)$ at the end of the phase transformation ($q = 1$). The corresponding bending moment is calculated by the formula $M = 0.274E_+I/l$, where I is the cross-sectional moment of inertia of the rod or a plate. To obtain a ring or a tube outside the phase-transformation interval, it is necessary to apply the moment $M = 2\pi E_+ I/l$ for the austenite phase and moment $M = 2\pi E_- I/l$ for the martensite phase.

Buckling of a Rod and a Plate under Axial Compression. We consider a two-hinged straight rod constrained against displacements at $t = 0$ and loaded in the austenite phase by a compressive force $T_3 = -P$ applied to the end $t = 1$. As in the previous case, there are no distributed external loads ($P_2 = P_3 = Q_1 = 0$) and $\theta_0 = 0$. System (20) is subjected to the following boundary conditions different from (22):

$$y_1(0) = 0, \quad y_2(0) = 0, \quad y_3(0) = 0, \quad y_1(1) = 0, \quad y_4(1) = 0, \quad y_5(1) = -p. \tag{23}$$

Here $p = Pl^3/(IE_0)$ is a numerical parameter of the end force.

The nonlinear boundary-value problem (20), (23) was analyzed numerically by the shooting method using the Mathcad software [5]. Branching of the solutions of the boundary-value problem was studied by varying the loading parameter p and the phase parameter q.

Figure 2 shows the branching of dependences of the parameters of state u and w on the loading parameter outside the phase-transformation interval for a rod with the geometrical parameter $\varepsilon = 0.02$ (u and w are the axial displacement of the free end and the maximum deflection, which are normalized to the rod length and expressed in percent). If the load is lower than the Euler critical load and the phase strains vanish, the rod remains straight ($w = 0$) in the deformed state. The branching is shown in the neighborhood of the Euler critical load $p \simeq 9.8$. For $p < 9.8$, the rod has only rectilinear shapes of equilibrium: $w = 0$, and the values of the parameter u are

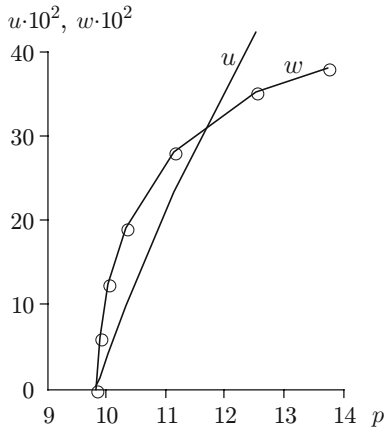

Fig. 2

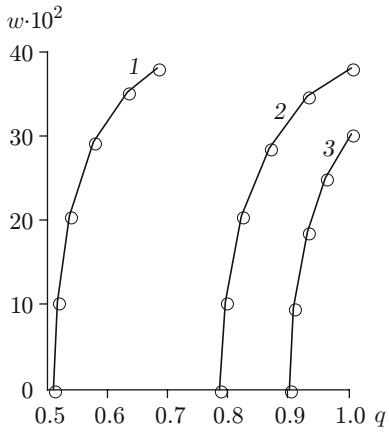

Fig. 3

Fig. 2. Parameters of state u and w versus the loading parameter p outside the phase-transformation interval.

Fig. 3. Dependence $w(q)$ in the phase-transformation interval for the loading parameter $p = 1.0$ (1), 0.6 (2), and 0.5 (3).

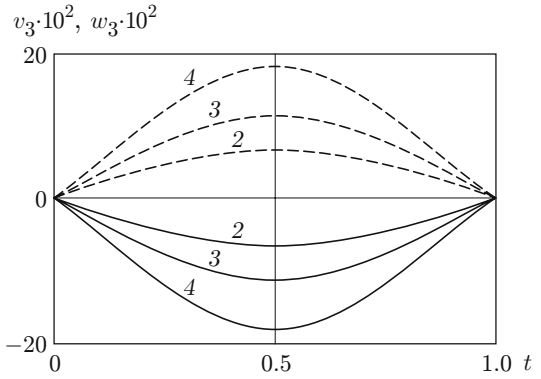

Fig. 4

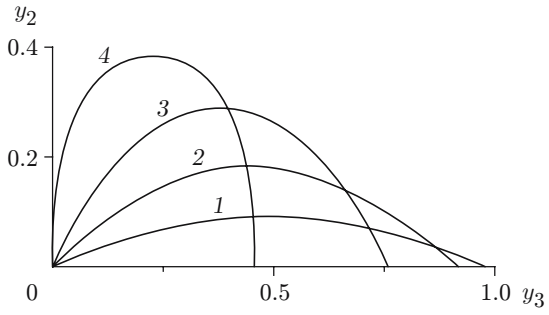

Fig. 5

Fig. 4. Strain distribution along the rod for different values of the parameter q (see Table 1): the solid curves refer to the total strains in the most compressed fiber of the rod, and the dashed curves refer to the bending strains.

Fig. 5. Curvilinear shapes of the rod for different values of the parameter q (see Table 1).

so small that, in the scale of Fig. 2, the corresponding line cannot be distinguished from the abscissa axis. In the neighborhood of the critical point, intense buckling of the rod occurs, and both parameters of state increase abruptly. The results shown in Fig. 2 correspond to the austenite and martensite phases of the rod. To calculate the physical force parameters in this case, one should take $E_0 = E_+$ for the austenite phase and $E_0 = E_-$ for the martensite phase.

The results of the analysis of the branching pattern in the phase-transformation interval are plotted in Fig. 3. The branches of the buckled states are shown for the loading parameter $p = 1.0$, 0.6, and 0.5 and different values of the phase parameter q. The buckling occurs at the point $q \simeq 0.507$ for $p = 1.0$, at $q \simeq 0.784$ for $p = 0.6$, and at $q \simeq 0.899$ for $p = 0.5$. In the neighborhood of the critical points, the deflections increase abruptly. The minimum value of the loading parameter for which the rod buckles due to the phase transformation is $p \simeq 0.43$.

For $p = 0.6$, more detailed data on the phase-strain evolution in the rod are listed in Table 1 and plotted in Figs. 4 and 5. Table 1 contains the values of the parameters u and w, the angles of rotation at the boundary point,

TABLE 1

Curve number in Figs. 4 and 5	q	u, %	w, %	$\theta(1)$	$\lvert u_{32}\rvert$, %	$\lvert u_{33}\rvert$, %	$\lvert v_{33}\rvert$, %	$\lvert w_{33}\rvert$, %
1	0.790	2.4635	9.0904	0.2873	0.1881	0.3979	3.1322	3.5301
2	0.811	9.0354	18.1850	0.5912	0.3828	0.4116	6.4819	6.8935
3	0.865	24.3790	28.7220	1.0017	0.6312	0.4482	11.1490	11.5970
4	1.000	55.1510	38.1960	1.5713	0.9296	0.5497	18.1820	18.7320

and the maximum values of the shear strains $|u_{32}|$ and $|u_{33}|$, bending strains $|v_{33}|$, and total strains $|w_{33}|$ for different values of the parameter q. The data of Table 1 show that the shear, bending, and total strains increase much faster than the compressive strain u_{33}; the transverse shear strain u_{32} reaches a maximum value at the boundary points, whereas the bending and total strains reach their maximum values in the middle cross section of the rod.

Figure 4 shows the strain distribution (in percent) along the rod for the corresponding values of q from Table 1. The curves that refer to the bending strain are shown above the abscissa axis, and the curves that refer to the total strain in the most compressed fiber of the rod are shown below the abscissa axis. An almost symmetrical location of the upper and lower curves about the abscissa axis shows that the shear strains are small compared to the bending strains (this conclusion follows also from the data of Table 1). In the alloy considered, the thermoelastic strains can be as high as 15%; therefore, the rod can undergo plastic strains or fail within the interval $0.865 < q < 1.000$.

Figure 5 shows the buckled shapes of the rod for the corresponding values of the parameter q from Table 1. In the unloaded austenite state, the rod corresponds to a unit interval on the abscissa axis.

Conclusions. A theoretical analysis of the results obtained shows that the phase transformation can have a considerable effect on the critical load in a wide range of external-load values. This fact can be used to find optimal technological solutions. Undoubtedly, the theoretical findings should be supported experimentally. Theoretical and experimental data may diverge for the following two most probable reasons. First, the physical properties of any alloy vary within a rather wide range. The second possible reason is the inadequacy of the mathematical model of the phase transformation. If the mathematical model is adequate, a theoretical analysis can be used to refine the physical constants of a real alloy. Otherwise, experimental data can be used to construct a more exact model of the phase transformation.

This work was supported by the Russian Foundation for Basic Research (Grant No. 04-01-00267).

REFERENCES

1. A. A. Movchan, "Micromechanical constitutive equations for shape-memory alloys," *Probl. Mashinostr. Nadezh. Mashin*, No. 6, 47–53 (1994).
2. A. A. Movchan, "Effect of variable elastic moduli and stresses on the phase content of shape-memory alloys," *Izv. Ross. Akad. Nauk, Mekh. Tverd. Tela*, No. 1, 79–90 (1998).
3. A. A. Movchan and A. N. Danilin, "Method for solving geometrically nonlinear problems of shape-memory-alloy rods for the direct transformation," *Probl. Mashinostr. Nadezh. Mashin*, No. 4, 83–90 (2002).
4. L. I. Shkutin, "Incremental deformation model for a rod," *J. Appl. Mech. Tech. Phys.*, **40**, No. 4, 757–762 (1999).
5. L. I. Shkutin, "Numerical analysis of the branched forms of bending for a rod," *J. Appl. Mech. Tech. Phys.*, **42**, No. 2, 310–315 (2001).